46th AIAA/ASME/SAE/ASEE Joint Propulsion Conference & Exhibit
25 - 28 July 2010, Nashville, TN

AIAA 2010-6545



# Gaseous Oxygen Injection Effects in Hybrid Labscale Rocket Motor Operations

Susane R. Gomes[1], Leopoldo Rocco Junior[2], José A. F. F. Rocco[3], and Koshun Iha[4]
*Aeronautical Institute of Technology, São José dos Campos, SP, 12228-901 and Flowtest Aerospace Research, Inc., Caieiras, SP, 07700-000*

**Hybrid rocket motor features such as operational safety, thrust tailoring, low investment cost and constructive simplicity are currently widespread. Nevertheless, inefficient combustion reduced mass fraction and mostly low regression rates still play a role in the major disadvantages. Swirling oxidizer flow is known to affect the mixing between oxidizer and fuel, intensifying heat exchange thus increasing regression rate. A laboratory scale hybrid engine was developed, and tests were conducted with gaseous oxygen (GOX) supply, ultra high molecular weight (UHMW) polyethylene, one axial and two swirl injector types. Oxygen mass flow, grain length and diameter and test time were maintained constant in order to evaluate the GOX injection influence on the motor performance and combustion characteristics. Series of six tests for each injector were performed with one unique set of machined throat diameters, to acquire a range of oxidizer mass flux for comparison. The data of oxidizer mass and fuel consumption were collected, and average regression rate values were calculated. Empirical correlations for the regression rate coefficients were obtained for each injection method. The burn grain profiles were analyzed and compared, sustaining that the income oxidizer flow pattern strongly affects the regression rates.**



## Nomenclature

| | | |
|---|---|---|
| $\dot{r}$: | = | regression rate of the solid fuel |
| $\bar{\dot{r}}$: | = | average fuel regression rate along the port |
| $a$ | = | regression-rate coefficient |
| $a_0$ | = | regression-rate coefficient incorporating grain length |
| $G$: | = | propellant mass flux rate |
| $\bar{G}$: | = | average propellant mass flux rate |
| $\bar{G}_{ox}$: | = | average oxidizer mass flux rate |
| $n$: | = | regression rate exponent |
| $m$: | = | regression rate exponent |
| $L_p$ | = | port length |
| $F$ | = | thrust magnitude |
| $g_0$ | = | local gravity value |
| $D_i$ | = | initial port diameter |
| $D_f$ | = | final port diameter |
| $\rho_f$ | = | fuel density |
| $\bar{\dot{m}}$ | = | propellant mass flow rate |
| $\bar{\dot{m}}_f$ | = | fuel mass flow rate |
| $\bar{\dot{m}}_{ox}$ | = | oxidizer mass flow rate |
| P | = | Chamber Pressure |
| O/F | = | Oxidizer to fuel ratio |
| Isp | = | Specific Impulse |

[1] Aeronautical Engineer and MSc Candidate, Chemistry Department, susaneribeiro@gmail.com , AIAA Student Member.
[2] Mechanical Engineer and PhD Candidate, Chemistry Department, flowtest@flowtest.com.br , and AIAA Student Member.
[3] Professor, Chemistry Department, friz@ita.br , AIAA Senior Member.
[4] Professor, Chemistry Department, koshun@ita.br , AIAA Senior Member.

$Isp_v$ = Specific Impulse
$\gamma$ = Isentropic Parameter
$c^*$ = Characteristic velocity

## I. Introduction

Humankind curiosity draws science farther century by century, and space exploration, a branch of this vast investigation, keeps fascinating individuals beyond borders. The endeavoring pursuit of chemical propulsion advancement is nowadays also focused on security issues, environmental friendliness and lower production costs. Amongst the propulsion possibilities, the hybrid rocket motors present not only the cited advantages as well as increased reliability and throttling capability.

However, despite the advantages, hybrid engines have inherent performance problems such as the low density specific impulse, poor combustion efficiency and reduced mass fraction[1]. Additionally, the regression rate values, thus the total mass flow and total thrust, are below the results produced by solid motors of similar size. Therefore, the phenomenon of hybrid rocket combustion has been subjected to theoretical and experimental investigation in the past decades.

Therefore, means to increase the hybrid combustion efficiency are necessary, and the regression rate becomes the fundamental parameter in the hybrid motor design. Hybrid combustion occurs as a macroscopic diffusion flame, and the zone is established within the boundary layer[2]. The regression rate depends primarily on the convective heat transfer from the flame to the fuel surface thus the whole combustion process will be affected severely by the incoming oxidizer flow pattern[3].

The research of techniques to increase the combustion efficiency drew the scientific community to the research of oxidizer injection methods, and it was verified that the entrance conditions affect severely the burn pattern. Our previous research[4] deals with projects and testing of injector configurations applied to liquid rocket motors. The studies comprised the inlet spray pattern, including spray cone-angle and spray injection velocity and droplet size. This time, axial and swirling injection modules were developed and tested in a labscale hybrid rocket environment, the performance parameters were compared and correlations between regression rates and oxidizer incoming flux were proposed.

The different aspects of the oxidizer injection effects on the combustion efficiency and fuel consumption shape are analyzed and compared. Moreover, it was verified that the swirling method increases the regression rates in the whole grain and particularly in the recirculation and impingement regions, due to the convective heat flux augmentation.

## II. Experimental setup

The baseline engine design was developed from a need for simplicity and flexibility; therefore a modular design was incorporated. The set could be assembled and disassembled in minutes allowing the practice of many tests per session.

The case and the flanges were made from stainless steel. The case was machined to fit between the steel flanges. The nozzle was adapted in the aft flange, to avoid nozzle exit during firings. A hydraulic system was settled to perform the thrust measurements. A schematic diagram of the test facility is exposed in Fig. 1. Compression fitting valves were used in the oxygen feed line. A pyrotechnic method was used to achieve ignition.

The chamber's length is 215 mm with an inner diameter of 68.3 mm. The grains are 195 mm long. The aft-chamber has a span of 15 mm and the pre-chamber is 5 mm long.

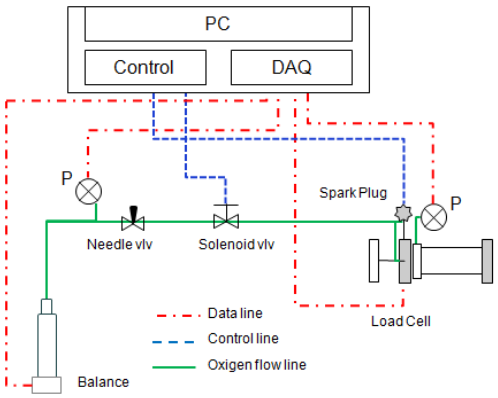


**Figure 1. Diagram of the experimental apparatus.**

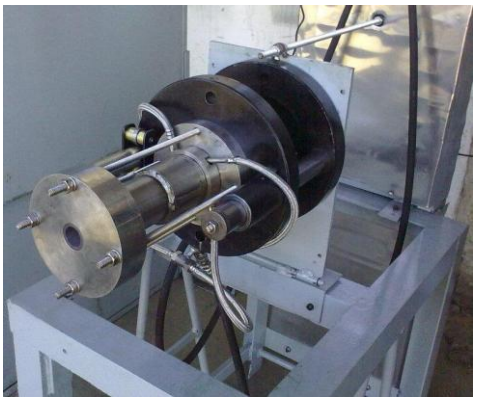

**Figure 2. Picture of the hybrid rocket motor configuration.**



## A. Injector geometries

Three injectors were developed, one axial and two swirls. On behalf of clarification, the swirling types will be distinguished by the allusion to the size, as the small and the large ones. The injectors can be used separately or combined. The basic characteristics of the systems are listed in Table 1.

Both injectors' combinations involving axial with swirl types present 5 exits, one from the axial and four from the swirl. The combined configurations differ in the number of entrances, once the large swirl has four entrances, and the small one has a single entry.

Table 1. Basic set configurations of single and combined injectors.

| Configuration | Injection method | Number of entrances | Exit diameter (mm) | Number of exits | Exit area ($mm^2$) |
|---|---|---|---|---|---|
| 1 | Axial | 1 | 3 | 1 | 7.07 |
| 2 | Small swirl | 1 | 1.5 | 4 | 7.07 |
| 3 | Large swirl | 4 | 1.5 | 4 | 7.07 |
| 4 | Axial + Small Swirl | 2 | - | 5 | 14.14 |
| 5 | Axial + Large swirl | 5 | - | 5 | 14.14 |

The following figures show pictures of different side views of the injectors. With the same setup, see Fig. 3 and 4, the axial or small swirl can be used, because there are separate hoses of oxygen supply connected to each injector as shown in Fig. 3. The easy interchange of injectors in the head flange and effortless alteration in the oxygen feed line due to the compression fit valves connections contribute to the trouble-free experimental apparatus.

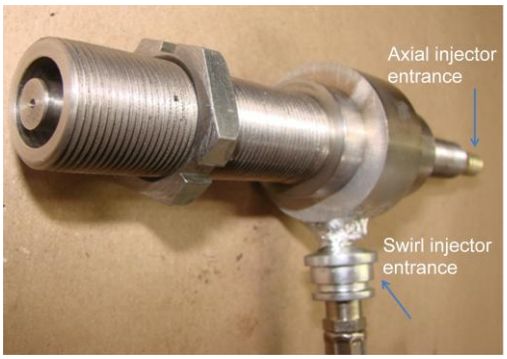


**Figure 3. Cross view of the injector with small swirl and axial exits with the two possible entrances and exits of oxidizer flux.**

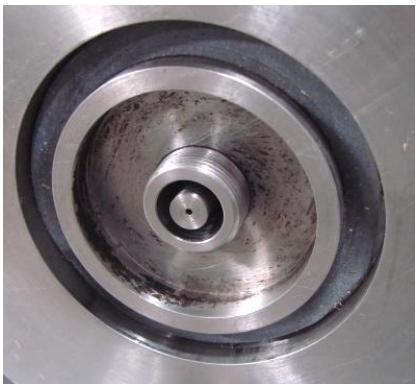

**Figure 4. Injector mounted in the test bench.**

FiguresFigure 4 and Figure **5** display the injectors attached to the head flange of the test bench. In Figure 5 the oxidizer supply hoses are already connected to the injector, whilst Fig. 6Figure 6 shows the lateral view of the large swirl alone.

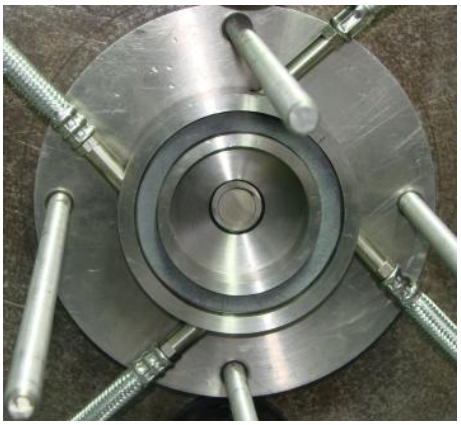

**Figure 5. Front view of the large swirl with the four oxidizer supply entrances.**

**Figure 6. Lateral view of the large view without the connectors and hoses.**

All injection exits and entrances are identical to guarantee homogeneous flow and regular burning along the port. The large injector outlet area works like a pre-chamber, enhancing the uniformity of the incoming flow conditions.

### B. Materials selection

Gaseous oxygen was used for its good performance, ease of handling, and costs. Two branches of polyethylene were tested for fuel grains, ultra high molecular weight (UHMW) and High Density Polyethylene (HDPE). The first tests evidenced that UHMW had better performance and did not produce excessive carbon black, which, in the HDPE tests, deposited even on the nozzle throat.

The first nozzle used was made of stainless steel. But it could not handle a 25 s test without throat enlargement and oxidation. Therefore, graphite (20 μm grain length) was used. The graphite could endure each test with a maximum throat growth of 0.5 mm.

Long tests were performed to address nozzle endurance during high temperature circumstances. As a result it as observed that the stainless steel around the nozzle and case suffered melting before problems could be noticeable on the nozzle, sustaining the quality of the graphite as a functional material for this application.

**Figure 7. Graphite nozzle surrounded by melted stainless steel, after a long firing test.**

The labscale motor design was based on the optimization obtained with the American Air Force Specific Code. The best oxidizer-to-fuel ratios for the pressures 10 and 15 atm were obtained. The optimum performance parameters are exhibited in Table 2. The nozzle was designed to produce a slightly over-expanded flow in the exit.

Table 2. Optimum performance values for UHMW Polyethylene and GOX combustion.

| P (atm) | 10 | 15 |
|---|---|---|
| O/F | 1,84 | 1,87 |
| Isp (s) | 229 | 245,8 |
| Isp vac (s) | 270 | 280,2 |
| $\gamma$ | 1,233 | 1,232 |
| $c^*$(m/s) | 1801 | 1813 |

## III. Results and discussion

### A. Regression rate analysis

Various authors proposed a regression mechanism based on the formation of a melting layer at the burning surface[5]. This layer is characterized by the presence of droplets of fuel entrained in the combustion zone along with the gasified fuel. One can then deduce that the surface tension and the melt layer viscosity may determine the fuel entrainment. High viscosity tension and high viscosity are known to reduce the regression rates, and this is the reason why polymers like Polyethylene and Plexiglas have lower regression rates. Therefore, the polyethylene will be the polymer used in this research once different conditions may improve the low performance of the fuel combustion.

Equation (1) represents the general form of the regression rate equation.

$$\dot{r} = aG^n x^m \tag{1}$$

Along the port, two competing effects are the source of fuel consumption uniformity. As the boundary layer, denoted by $x^m$, increases, heat flux decreases, nevertheless at the same time the total mass flux increases due to the gasified fuel. Therefore, the regression rate may be expressed in terms of average values[1], as follows.

$$\dot{r}_{avg} = aG_{avg}^n L_p^m \tag{2}$$

Since the ballistic parameters depend on the mass flux, researchers found more opportune, and with reasonable precision, to use the simplified burning expression, Eq. (3), for a given motor length and constant mass flow rate[1].

$$\dot{r}_{avg} = a_0 \bar{G}_{ox}^n \tag{3}$$

### B. Data reduction

The key purpose of the regression rate analysis is to determine the correlation between regression rates and easily controlled parameters along with experimentally derived constants. Correlation patterns were determined by making scatter plots and applying correlation analysis to the cluster of data points provided by the test firings.

The average regression rate was calculated as follows[3]

$$\bar{\dot{r}} = \frac{\bar{\dot{m}}_f}{\pi\left(\frac{D_i + D_f}{2}\right) L_p \rho_f} \tag{4}$$

The average oxygen mass flux equation considers the area associated to the medium diameter

$$\bar{G}_{ox} = \frac{4\bar{\dot{m}}_{ox}}{\pi\left(\frac{D_i + D_f}{2}\right)^2} \tag{5}$$

The medium propellant mass flow rate was calculated considering the mass of fuel and oxygen used.

$$\bar{\dot{m}} = \bar{\dot{m}}_f + \bar{\dot{m}}_{ox} \tag{6}$$

The $I_{sp}$ values were obtained from the thrust data collected in the tests.

$$I_{sp} = \frac{F}{\bar{\dot{m}} g_0} \tag{7}$$

### C. Performance parameters comparison between different injection methods.

The results of the three series of four tests are exposed in Table 3.

**Table 3. Experimental regression rates and fluxes collected in the four firing tests of each injector.**

| Injector type | $\dot{r}$ (mm/s) | $\bar{G}_{ox}$ $(kg/m^2s)$ | $\dot{r}$ (mm/s) | $\bar{G}_{ox}$ $(kg/m^2s)$ | $\dot{r}$ (mm/s) | $\bar{G}_{ox}$ $(kg/m^2s)$ | $\dot{r}$ (mm/s) | $\bar{G}_{ox}$ $(kg/m^2s)$ |
|---|---|---|---|---|---|---|---|---|
| Axial | 0,39 | 53,6 | 0,38 | 53 | 0,37 | 42,0 | 0,27 | 16,2 |
| Large Swirl | 0,55 | 40,3 | 0,52 | 34,1 | 0,32 | 11,4 | 0,21 | 4,5 |
| Small Swirl | 0,45 | 45,1 | 0,41 | 50,4 | 0,22 | 19,6 | 0,17 | 6,11 |

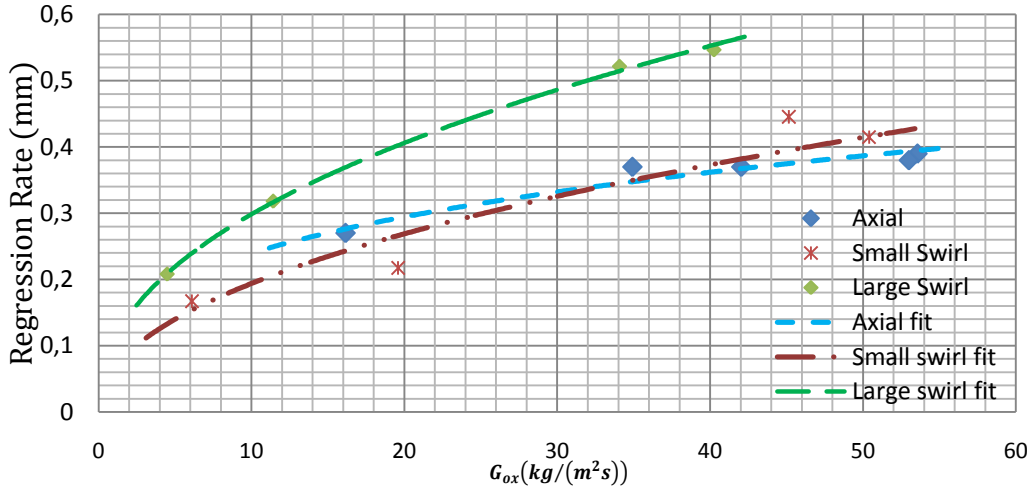


**Figure 8. Regression rate versus oxidizer mass flux for each injection method.**

**Table 4. Experimental regression rate constants.**

| Injector | $a_0$ | n | $R^2$ |
|---|---|---|---|
| Axial | 0,121 | 0,30 | 0,936 |
| Small swirl | 0,065 | 0,47 | 0,961 |
| Large Swirl | 0,107 | 0,45 | 0,999 |

The diffusion-controlled model assumed that reaction rates are faster than the diffusion rates and that the boundary layer is much larger than the combustion zone. But it is observed that, at constant pressure, when mass flux decreases the regression is likely to deform and depend on the radiation environment, becoming larger than the extrapolated values[1,3]. Differently, at high mass fluxes or low pressure, turbulence diffusion rates can dominate and reaction rates, which are influenced by pressure, become rate determining. Thus, the regression rates goes down the extrapolated values.

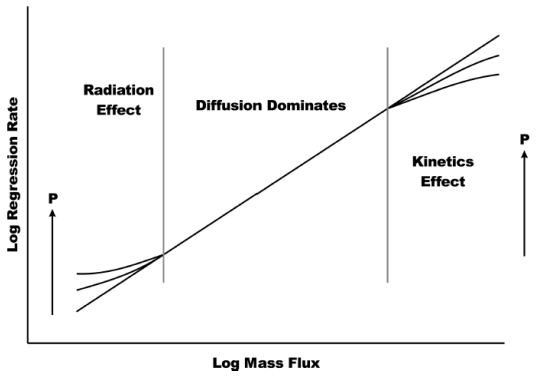


**Figure 9. Diagram of the influence of radiation and kinetics effects on regression rates.**

The experimentally determined constant n does not depend on heat transfer, accordingly as the heat exchange increases n decreases, in parallel the kinetic case also reduces n. Therefore, the higher values are obtained in situations where diffusion dominates.

The following graph, Fig. 10, shows the data dispersion with smooth lines. All the curves resemble the patch of Fig. 9 associated with diffusion domination. The values of the constant *n* obtained sustain this affirmation.

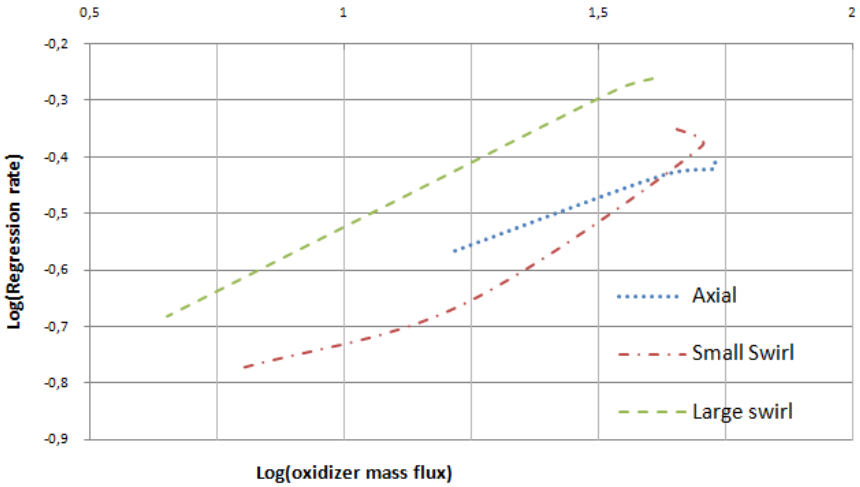


**Figure 10. Scatted data with smooth lines.**

The coefficient "a" contains the properties of the combustion gas, and depends on the flow dynamics. Therefore, as expected by the theory, the higher constant was resulted from the large swirl case, due to the better flow characteristics.

The Table 4 presents the best performance parameters obtained in the firings for each injection method. The larger swirl provided the best results in all judgments even when compared to the combination of swirl methods.

**Table 5. Performance comparison of the best parameters obtained for each injection configuration.**

| Injector type | $\dot{r}$ (mm/s) | Thrust (N) | Isp (s) | $\bar{G}_{ox}(kg/m^2s)$ |
|---|---|---|---|---|
| Axial | 0,39 | 55,1 | 134 | 53,6 |
| Large Swirl | 0,55 | 75,0 | 195 | 40,3 |
| Small Swirl | 0,45 | 73,9 | 187 | 45,1 |
| Large Swirl + Axial | 0,50 | 73,5 | 185 | 41,04 |
| Small Swirl + Axial | 0,43 | 63,8 | 160 | 42,1 |

From the data collected it was clear that higher pressures produce more stability and the tests become more repeatable. The thrust also appears to be steadier when the supply pressure is high.

### D. Grain analysis

From the experiments with different grains, diverse grain profiles were obtained. The following discussion investigates how the injection methods affect the performance parameters. The subsequent picture, Fig. 11, is a grain used with the axial injector. The primary remark is the irregular burn profile along the longitudinal axis, the regression rate presents a maximum at about 25% of the grains' length, and then the consumption keeps decreasing until the aft end.

**Figure 11. Grain cross section after axial injector test.**

The next observation is the flow pattern observed on the grain surface of small swirl tests. The rotating entrance conditions can be seen by the helicoidally disposed curves on the surface, Fig. 12 and 13.

**Figure 12. Helicoidally disposed curves on the grain surface subsequent to small swirling injector test.**

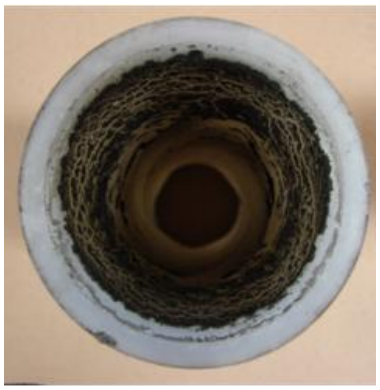

**Figure 13. Grain superior view obtained from the small swirl injector test.**

As experimentally observed in Fig. 12, the regression rates achieved in the beginning of the grain are the highest values. This region is usually called impingement zone due to the strong influence of the incoming rotating flow[6]. The high angular moment enhance the heat exchange which magnifies the velocity of fuel degradation or pyrolisis. However, the excessive carbon black in the cavity close to the head end means that there was a lack of oxidizer or the residence time, in this region, was insufficient for complete combustion.

The following analysis, Fig. 14 and 15, regards the union of two different injector methods. The axial was used in parallel with the small swirl injector, as showed before in Fig. 4. It is shown that one side was more consumed than the other; which means that the flow inside the chamber probably has high instability. The photos resemble a fusion between the pos-combustion grains obtained via axial and small swirl injection methods separately.

**Figure 14. Grain cross section after axial combined with small swirling injectors test.**

**Figure 15. Grain superior view. Helicoidally disposed imprints along the axis obtained after axial and small swirling injectors test.**

Subsequently, the grains obtained in the large swirl firings are shown.

**Figure 16. Grain cross sectional view after large swirl firings.**

**Figure 17. Helicoidally consumption pattern after a typical large swirl test firing.**

Experimental investigations have shown that the controlling factors in the combustion process are the rate of heat transfer to the solid surface and the heat of decomposition of the solid-phase fuel[3]. The mass flux, which is regulated by the rate of flow of the liquid phase, determines the rate of heat generated in the combustion zone and hence determines both the heat transfer and the thrust magnitude.

The oxidizer flow condition on the fuel surface causes the turbulent diffusion flame which in turn affects the heat transfer increasing the regression rate. Therefore, the better mixing originated by the swirl increases the combustion efficiency and fuel consumption. This imply that the fuel propellant mass flow rate, and in turn, the total propellant mass flow, is controlled by the combustion efficiency in the combustion chamber as suggested by Yuasa and coworkers[6].

The helicoidally form of the fuel grains after firings shows quite clearly the flow pattern over the surface. Regions with high angular momentum, particularly on the head end, present high regression rates.

The flow from the swirling type injector enters the combustion chamber with a centrifugal force; this condition is responsible for the high oxygen flow velocity, particularly the tangential component, and the augment of the density near the surface. These summing effects plus the amplified residence time account for the boundary layer shrink and, therefore, the enhancement of the burn rates.

The grain observation, , supports the superiority of the large swirl already evidenced by the collected data, because the deposit of carbon black on the surface and on the nozzle entrance was by far the least, due to the augment of the residence time, and the regression rates were the largest.

In all tests, the lower end of the grain presented quite smaller regression rates than those from other cross sections, which is explained by the radiant heat transfer phenomenon dominant in this region due to the higher total mass flux[1].

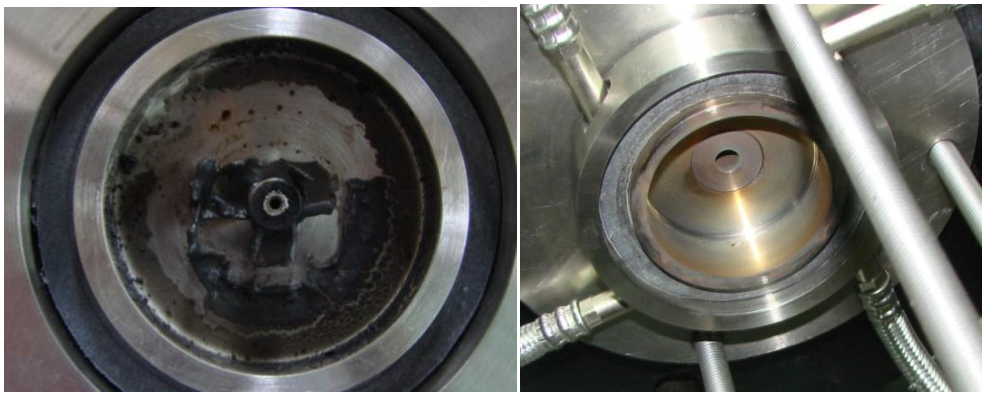

**Figure 18. Comparison between injector cross-section after firings, axial test (left) and large swirl test (right).**

All tests with axial injector affected the injector material as shown in Fig. 18, it was necessary the integration of a long pre-chamber. The flow downstream the injector exit forms a recirculation zone

which blocks heat transfer from the flame to the bulk head, therefore there is no need for insulation in the swirl case. The same barrier effect was obtained and documented by Jones and coworkers[8].

### E. Plume pattern

The slightly over-expanded flow was obtained in most tests. And this phenomenon confirms that the exit pressure is less than ambient pressure; therefore, the exhaust stream contracts and a pattern of Mach diamonds appears, Fig. 19. The small exit pressures devise the conformity of the project with higher design altitudes.

**Figure 19. Mach diamond pattern along the plume.**

## IV. Conclusions

The main objective of this research was to evaluate and compare the regression rates of polyethylene fuel grains under three different oxidizer injection methods. The thrust and specific impulse were also obtained, but mechanical issues produced poor results, which caused significant scatter in the thrust data, and consequently in the specific impulse records.

A technique to increase the regression rates of polyethylene fuel grains using different income oxidizer flow conditions was proposed. Two swirl and one axial injector types were tested and the performance obtained was recorded and compared. The swirl injectors produced better conditions than the axial, which were in accordance with the literature data[9]. The larger swirl provided an even better outcome in the regression rates, thrust and specific impulse.

The non uniform port diameter obtained in burned grains sustain that regression rate strongly depend on the income oxidizer flow pattern. Therefore, applying swirl to the oxygen jet improves low performance of the hybrid fuel combustion as proposed in the literature[6,7]. However, future research should verify how the combustion pattern changes in different system scales, once this effect is not yet renowned and quantified but is essential for design of hybrid rocket motors based on labscale tests.

## Acknowledgments

The authors gratefully acknowledge financial support from CNPq (Conselho Nacional de Desenvolvimento Científico e Tecnológico).

## References

[1]Altman, D., and Humble, R. (1995). "Hybrid rocket propulsion systems," In "Space Propulsion Analysis and Design" (R. Humble, G. Henry, and W. Larson, eds.), pp. 365–441, McGraw-Hill, New York.)

[2]Marxman, G.A. and Gilbert, G.M., "Turbulent boundary layer combustion in the hybrid rocket", Ninth Symposium (Intern.) on Combustion, the Combustion Institute, 1963, pp. 371-383.

[3]Altman, D., Rocket Motors, Hybrid. The Encyclopedia of Physical Science and Technology. Vol. 14, 2001. ISBN: 978-0-12-227410-7.

[4]Rocco, J., A., Rocco, L., Gonçalves, R., Iha, K., "Studies on a Pressurized Swirl Injector Bi-Propellant Used in Rocket-Motor", 45th AIAA/ASME/SAE/ASEE Joint Propulsion Conference and Exhibit, Denver, Colorado, Aug. 2-5, 2009. AIAA -2009-5494.

[5]De Zilwa, S., Zilliac, G., Karabeyoglu, M A and Reinath, M., "Time-Resolved Fuel-Grain Measurement in Hybrid Rockets", AIAA Paper 2003-4595 , July 2003.

[6]Imamura, T., Shimada, O., and Yuasa, S., "Effects of Swirling Oxygen Flow on the Performance of a Hybrid Rocket Engine," Proceedings of the 36"' Conference on Aerospace Propulsion, Japan Sot. Aero. Space Sci., 1996, pp.303-308 (in Japanese).

[7]Knuth, W.H. et al., "Experimental Investigation of a Vortex-Driven High-Regression Rate Hybrid rocket Engine," AIAA Paper 98-3348, 1998.

[8]Jones, C. C., Myre, D. D., Cowart, J. S., "Performance and Analysis of Vortex Oxidizer Injection in a Hybrid Rocket Motor" , AIAA Paper 2009-4938, 45th AIAA/ASME/SAE/ASEE Joint Propulsion Conference and Exhibit, Denver, Colorado.

[9]Carmicino, C., and Russo Sorge, A, "Investigation of the Fuel Regression Rate dependence on Oxidizer Injection and Chamber Pressure in a Hybrid Rocket," AIAA Paper 2003-4591.